

High-Resolution Spiral Computed Tomography Coronary Angiography in Patients Referred for Diagnostic Conventional Coronary Angiography

Nico R. Mollet, MD; Filippo Cademartiri, MD; Carlos A.G. van Mieghem, MD; Giuseppe Runza, MD; Eugène P. McFadden, MB, FRCP; Timo Baks, MD; Patrick W. Serruys, MD; Gabriel P. Krestin, MD; Pim J. de Feyter, MD

Background—The diagnostic performance of the latest 64-slice CT scanner, with increased temporal (165 ms) and spatial (0.4 mm³) resolution, to detect significant stenoses in the clinically relevant coronary tree is unknown.

Methods and Results—We studied 52 patients (34 men; mean age, 59.6±12.1 years) with atypical chest pain, stable or unstable angina pectoris, or non-ST-segment elevation myocardial infarction scheduled for diagnostic conventional coronary angiography. All patients had stable sinus rhythm. Patients with initial heart rates ≥70 bpm received β-blockers. Mean scan time was 13.3±0.9 seconds. The CT scans were analyzed by 2 observers unaware of the results of invasive coronary angiography, which was used as the standard of reference. All available coronary segments, regardless of size, were included in the evaluation. Lesions with ≥50 luminal narrowing were considered significant stenoses. Invasive coronary angiography demonstrated the absence of significant disease in 25% (13 of 52), single-vessel disease in 31% (16 of 52), and multivessel disease in 45% (23 of 52) of patients. One unsuccessful CT scan was classified as inconclusive. Ninety-four significant stenoses were present in the remaining 51 patients. Sensitivity, specificity, and positive and negative predictive values of CT for detecting significant stenoses on a segment-by-segment analysis were 99% (93 of 94; 95% CI, 94 to 99), 95% (601 of 631; 95% CI, 93 to 96), 76% (93 of 123; 95% CI, 67 to 89), and 99% (601 of 602; 95% CI, 99 to 100), respectively.

Conclusions—Noninvasive 64-slice CT coronary angiography accurately detects coronary stenoses in patients in sinus rhythm and presenting with atypical chest pain, stable or unstable angina, or non-ST-segment elevation myocardial infarction. (*Circulation*. 2005;112:2318-2323.)

Key Words: angina ■ angiography ■ coronary disease ■ imaging ■ tomography

Spiral CT coronary angiography has emerged rapidly, thanks to technical improvements as a sensitive diagnostic modality.¹⁻¹² The newest-generation spiral CT scanners are significantly improved. They feature 64 slices and thinner detectors, and the x-ray tube permits higher x-ray output and faster tube rotation. These improvements result in high-quality, nearly motion-free, isotropic image quality. Data are acquired during a single breathhold of ≈13 seconds. We report the diagnostic performance of 64-slice CT coronary angiography in 52 patients with atypical chest pain, stable or unstable angina, or non-ST-segment elevation myocardial infarction referred for diagnostic invasive coronary angiography to assess the extent and severity of coronary stenoses in the clinically relevant coronary tree.

Editorial p 2222

Methods

Study Population

During a period of 6 weeks, we studied 70 consecutive patients scheduled for diagnostic conventional coronary angiography who fulfilled the following criteria: sinus heart rhythm, able to hold breath for 15 seconds, and no previous percutaneous coronary intervention or coronary bypass surgery. Eighteen patients were excluded because of the logistical inability to perform a CT scan before the conventional angiogram (n=9), presence of arrhythmia (n=4), impaired renal function (serum creatinine >120 mmol/L) (n=4), and known contrast allergy (n=1). Thus, the study population comprised 52 patients (34 men; mean age, 59.6±12.1 years). Our institutional review board approved the study protocol, and all patients gave informed consent.

Received January 4, 2005; revision received June 23, 2005; accepted June 24, 2005.

From the Erasmus Medical Center, Departments of Cardiology (N.R.M., F.C., C.A.G.v.M., E.P.M., T.B., P.W.S., P.J.d.F.) and Radiology (N.R.M., F.C., C.A.G.v.M., G.R., T.B., G.P.K., P.J.d.F.), Rotterdam, the Netherlands.

Correspondence to P.J. de Feyter, MD, PhD, Erasmus Medical Center, Thoraxcenter, Room Bd-410, Dr Molewaterplein 40, 3015GD Rotterdam, Netherlands. E-mail p.j.defeyter@erasmusmc.nl

© 2005 American Heart Association, Inc.

Circulation is available at <http://www.circulationaha.org>

DOI: 10.1161/CIRCULATIONAHA.105.533471

Patient Preparation

Patients with heart rates >70 bpm received, unless they had known overt heart failure or ECG AV conduction abnormalities, a single oral dose of 100 mg metoprolol 45 minutes before the scan. Patients with heart rates >80 bpm received an additional single oral dose of 1 mg lorazepam.

Scan Protocol and Image Reconstruction

All patients were scanned with a 64-slice CT scanner (Sensation 64, Siemens) equipped with a new feature in multislice CT technology, so-called *z*-axis flying-focus technology.¹³ The central 32 detector rows acquire 0.6-mm slices, and the flying-focus spot switches back and forth between 2 *z* positions between each reading. Two slices per detector row are acquired, which results in a higher oversampling rate in the *z* axis, thereby reducing artifacts related to the spiral acquisition and improving spatial resolution down to 0.4 mm.¹³ Angiographic scan parameters included the following: number of slices per rotation, 32×2; individual detector width, 0.6 mm; rotation time, 330 ms; table feed, 3.8 mm per rotation; tube voltage, 120 kV; tube current, 900 mA; and prospective x-ray tube modulation, none. Calcium scoring parameters (similar unless indicated) were a tube current of 150 mA and prospective x-ray tube modulation. The radiation exposure for CT coronary angiography with this scan protocol was calculated as 15.2 to 21.4 mSv (for men and women, respectively) using dedicated software (WinDose, Institute of Medical Physics). The radiation exposure of calcium scoring using a comparable scan protocol (including prospective x-ray tube modulation) on a 16-slice scanner was calculated as 1.3 to 1.7 mSv (for men and women, respectively).¹⁴

A bolus of 100 mL contrast material (iomeprol, Iomeron 400) was injected through an arm vein at a flow rate of 5 mL/s. A bolus-tracking technique was used to synchronize the arrival of contrast in the coronary arteries with the initiation of the scan. To monitor the arrival of contrast material, axial scans were obtained at the level of the ascending aorta with a delay of 10 seconds after the start of the contrast injection. The scan was automatically started when a threshold of 100 Hounsfield units was reached in a region of interest positioned in the ascending aorta.

Images were reconstructed with ECG gating to obtain optimal, motion-free image quality. Data sets were reconstructed immediately after the scan following a stepwise pattern. Initially, a single data set was reconstructed during the mid- to end-diastolic phase (350 ms before the next R wave). Image quality was assessed on a per-segment level. In case of insufficient image quality of ≥1 coronary segments, additional data sets were reconstructed (300, 400, and 450 ms before the next R wave). In case of persistent artifacts related to coronary motion, a second reconstruction approach was carried out, including reconstruction of data sets during both the mid- to end-diastolic phase (between 60% and 70% of the R-R interval) and the end-systolic phase (between 25% and 35% of the R-R interval). If necessary, multiple data sets of a single patient were used separately to obtain optimal image quality of all available coronary segments. The reconstruction algorithm uses data from a single heartbeat obtained during half-x-ray tube rotation, resulting in a temporal resolution of 165 ms.

Quantitative Coronary Angiography

All scans were performed within 2 weeks of the conventional diagnostic angiogram. A single observer unaware of the multislice CT results identified coronary segments using a 17-segment modified AHA classification¹⁵ (right coronary artery: 1, proximal; 2, mid; 3, distal; 4a, posterior descending; 4b, posterolateral; left main coronary artery: 5, left anterior descending coronary artery (LAD); 6, proximal; 7, mid; 8, distal; 9, first diagonal; 10, second diagonal; circumflex coronary artery: 11, proximal; 12, first marginal; 13, mid; 14, second marginal; 15, distal; and 16, intermediate branch). All segments, regardless of size, were included for comparison with CT coronary angiography. Segments were classified as normal (smooth parallel or tapering borders), as having nonsignificant disease (luminal irregularities or <50% stenosis), or as having significant steno-

ses. Stenoses were evaluated in 2 orthogonal views and classified as significant if the mean lumen diameter reduction was ≥50% using a validated quantitative coronary angiography (QCA) algorithm (CAAS, Pie Medical).

CT Image Evaluation

All scans were analyzed independently by a radiologist and a cardiologist who were unaware of the results of conventional coronary angiography and used an offline workstation (Leonardo, Siemens). Total calcium scores of all patients were calculated with dedicated software and expressed as Agatston scores. The Agatston score is a commonly used scoring method that calculates the total amount of calcium on the basis of the number, areas, and peak Hounsfield units of the detected calcified lesions.¹⁶

All available coronary segments were visually scored for the presence of significant stenosis. Maximum-intensity projections were used to identify coronary lesions and (curved) multiplanar reconstructions to classify lesions as significant or nonsignificant. Disagreement between observers was resolved by consensus.

Image quality was evaluated on a per-segment basis and classified as good (defined as the absence of any image-degrading artifacts related to motion, calcification, or noise), adequate (presence of image-degrading artifacts but evaluation possible with moderate confidence), or poor (presence of image-degrading artifacts and evaluation possible only with low confidence).

Statistical Analysis

The diagnostic performance of CT coronary angiography for the detection of significant lesions in coronary arteries with QCA as the standard of reference is presented as sensitivity, specificity, positive and negative predictive values and positive and negative likelihood ratios with the corresponding exact 95% CIs. Comparison between CT coronary angiography and QCA was performed on 3 levels: segment by segment, vessel by vessel (no or any disease per vessel), and patient by patient (no or any disease per patient). We performed an additional sensitivity analysis after random selection of a single segment per patient to explore the effect of nesting; repeated assessments (segment by segment and vessel by vessel) within the same patient were made that were not independent observations. Intraobserver and interobserver variability for the detection of significant coronary stenosis was determined by κ statistics.

TABLE 1. Patient Characteristics

Symptoms	
Atypical chest pain	6 (12)
Stable angina pectoris	32 (63)
Unstable angina pectoris	3 (6)
Non-ST-segment elevation myocardial infarction	11 (22)
Risk factors	
Hypertension	17 (33)
Hypercholesterolemia	36 (71)
Diabetes mellitus	7 (14)
Smoking	15 (29)
Family history of acute coronary syndrome	13 (26)
Obese (body mass index ≥30 kg/m ²)	14 (28)
Calcium score, median (interquartile range)*	231 (15–736)
Conventional angiography	
Absence of coronary artery disease	7 (13)
Nonsignificant disease	6 (12)
Single-vessel disease	16 (31)
Multivessel disease	23 (45)

n=52. Values are n (%) unless otherwise indicated.

*Agatston score.

TABLE 2. Diagnostic Performance and Predictive Value of 64-Slice CT Coronary Angiography for the Detection of $\geq 50\%$ Stenoses on QCA

	n	Sensitivity, %	Specificity, %	PPV, %	NPV, %	+LR	-LR
Segment-based analysis							
All segments	725	99 (94–98)	95 (93–96)	76 (67–89)	100 (99–100)	20.81	0.01
Proximal segments	204	100 (89–100)	97 (93–98)	83 (67–97)	100 (97–100)	29.00	0.00
Mid segments	142	97 (83–99)	94 (88–97)	81 (63–96)	99 (94–99)	15.47	0.04
Distal segments	121	100 (68–100)	97 (92–99)	73 (39–98)	100 (96–100)	37.67	0.00
Side branches	258	100 (87–100)	94 (90–96)	65 (48–85)	100 (98–100)	16.57	0.00
LM	51	100 (21–100)	100 (93–100)	100 (92–100)	100 (2–100)	∞	0.00
LAD	230	97 (85–100)	92 (88–95)	69 (53–86)	99 (96–99)	12.68	0.03
LCx	235	100 (88–100)	97 (94–99)	83 (66–97)	100 (98–100)	34.33	0.00
RCA	209	100 (89–100)	95 (91–97)	77 (60–95)	100 (97–100)	19.89	0.00
Patient-based analysis							
All segments	51	100 (91–100)	92 (67–99)	97 (86–99)	100 (73–100)	13.00	0.00

PPV indicates positive predictive value; NPV, negative predictive value; +LR, positive likelihood ratio; -LR, negative likelihood ratio; LM, left main coronary artery; LCx, circumflex coronary artery; and RCA, right coronary artery. For segment-based analysis, analysis of 725 segments visualized on the conventional angiogram and classified according to a 17-segment modified AHA classification was performed. Segments were further classified on the basis of their location within the coronary tree (proximal, mid, or distal segments of the main coronary artery arteries or side branches) and their location within a single vessel (LM, LAD, LCx, or RCA). For patient-based analysis, analysis of 51 patients was performed. Values in parentheses represent 95% CIs.

Results

Patient characteristics are shown in Table 1. Seventy-three percent of the patients (38 of 52) received a β -blocker; 31% (16 of 52) also received lorazepam. The mean heart rate in these patients dropped within 45 minutes from 68.2 ± 10.2 to 57.8 ± 6.8 bpm. The mean scan time was 13.3 ± 0.6 seconds. One unsuccessful CT scan was classified as inconclusive because the development of ventricular bigeminy during the angiography scan.

A single data set for the assessment of significant stenoses was used in 69%, 2 data sets were used in 27%, and 3 data sets were used in 4% of patients to obtain optimal image quality of on a per-segment level. Data sets reconstructed during the end-systolic phase were used in 27% of patients (14/51). Image quality was classified as good in 90%, moderate in 7%, and poor in 3% of coronary segments. Reasons for poor image quality were motion artifacts (60%, 12 of 20), severe calcifications (20%, 4 of 20), or low contrast-to-noise ratio (20%, 4 of 20).

Diagnostic Performance of 64-Slice CT Coronary Angiography: Segment-by-Segment Analysis

A total, 725 segments were included for comparison with QCA. Potentially, 17 segments per patient can be present for

analysis. However, 142 segments were not visualized on the conventional angiogram because of variations in coronary anatomy (absence of an intermediate branch or hypoplastic, nondominant coronary arteries in which not all segments could be identified; 102 segments) and the presence of a proximal occlusion and poorly filled distal segments by collaterals (40 segments).

Interobserver and intraobserver variability for detection of significant lesions had κ values of 0.73 and 0.79, respectively. The diagnostic performance of CT coronary angiography for detecting significant lesions on a segment-based analysis is detailed in Table 2. One significant stenosis (lumen diameter reduction, 52%) located at the mid part of the LAD was detected with CT, but the severity of the stenosis was underestimated and classified as nonsignificant. Thirty nonsignificant lesions were detected with CT, but the severity of these stenoses was overestimated, resulting in incorrect classification as significant stenoses on the CT scan. Conventional angiography revealed only wall irregularities in 8 and nonsignificant stenoses in the remaining 22 lesions (mean lumen reduction, $34.7 \pm 7.9\%$; range, 23% to 49%). The vast majority (83%, 25 of 30) of these segments were calcified. The presence of coronary calcium induced overes-

TABLE 3. Influence of Coronary Calcification on Diagnostic Accuracy of 64-Slice CT Coronary Angiography on a Segment-Based Analysis

Calcium Score	n	Mean (\pm SD)				Sensitivity, %	Specificity, %	Positive PV, %	Negative PV, %	
		Agatston Score	TP	TN	FP					FN
0–10	12	0 \pm 0	8	171	2	0	100 (63–100)	99 (95–99)	80 (44–98)	100 (97–100)
11–400	21	174 \pm 122	36	240	13	0	100 (90–100)	95 (91–97)	73 (58–88)	100 (98–100)
401–1000	12	718 \pm 166	31	129	10	1	97 (83–98)	93 (87–96)	76 (59–89)	99 (95–99)
>1000	6	1731 \pm 621	18	61	5	0	100 (81–100)	92 (83–97)	78 (56–96)	100 (94–100)

TP indicates true positive; TN, true negative; FP, false positive; FN, false negative; and PV, predictive value. Values in parentheses represent 95% CIs.

timation of the severity of these lesions on the CT scan (Table 3). Agreement between CT coronary angiography and QCA on a per-segment level was very good (κ value, 0.83).

After random selection of a single segment per patient, the sensitivity for detecting significantly diseased vessels was 100% (13 of 13; 95% CI, 75 to 100), specificity was 95% (36 of 38; 95% CI, 82 to 99), positive predictive value was 87% (13 of 15; 95% CI, 59 to 99), and negative predictive value was 100% (36 of 36; 95% CI, 90 to 100).

Diagnostic Performance of 64-Slice CT Coronary Angiography: Vessel-by-Vessel Analysis

The diagnostic performance of CT coronary angiography for detecting significant lesions on a vessel-based analysis is detailed in Table 2. One significantly diseased LAD was incorrectly classified as nonsignificantly diseased on the CT scan. Sensitivity for the detection of significantly diseased LADs was 96% and 100% in all other main coronary arteries. Agreement between CT coronary angiography and QCA on a per-vessel level was very good (κ value, 0.85).

Diagnostic Performance of 64-Slice CT Coronary Angiography: Patient-by-Patient Analysis

The diagnostic performance of CT coronary angiography for detecting significant lesions on a patient-based analysis is detailed in Table 2. Twelve patients with either an angiographically normal coronary angiogram⁷ or nonsignificant disease⁵ were correctly identified with CT. However, 1 patient with only wall irregularities on the conventional angiogram was incorrectly classified as having single-vessel disease on the CT scan. All 38 patients with significant coronary artery disease on conventional angiography were correctly identified on the CT scan (Figures 1 and 2). However, in 7 patients with single-vessel disease also, another lesion was detected and its severity was overestimated, which resulted in incorrect classification as multivessel disease on CT coronary angiography. Agreement between CT coronary angiography and QCA on a per-patient (no or any disease) level was very good (κ value, 0.95); agreement between both techniques for classifying patients as having no, single-vessel, or multivessel disease was good (κ value, 0.72).

Discussion

Recent reports demonstrated that earlier-generation multislice CT scanners showed promise for noninvasive detection of coronary stenoses.¹⁻¹² The reported diagnostic values were high, but one should bear in mind that the calculated sensitivity and specificity were based on analyzable coronary segments rather than on all examined coronary segments. In fact, the most recent reports of 16-slice CT coronary angiography excluded 6% to 17% of the available coronary segments, and only a few included all available segments. In addition, only the larger parts of the coronary tree were examined; smaller parts with a diameter of <1.5 or 2 mm were excluded from analysis. Most recently, Leschka et al¹⁷ presented the first study exploring the diagnostic performance of 64-slice CT coronary angiography. They evaluated all available coronary segments ≥ 1.5 mm and reported a high

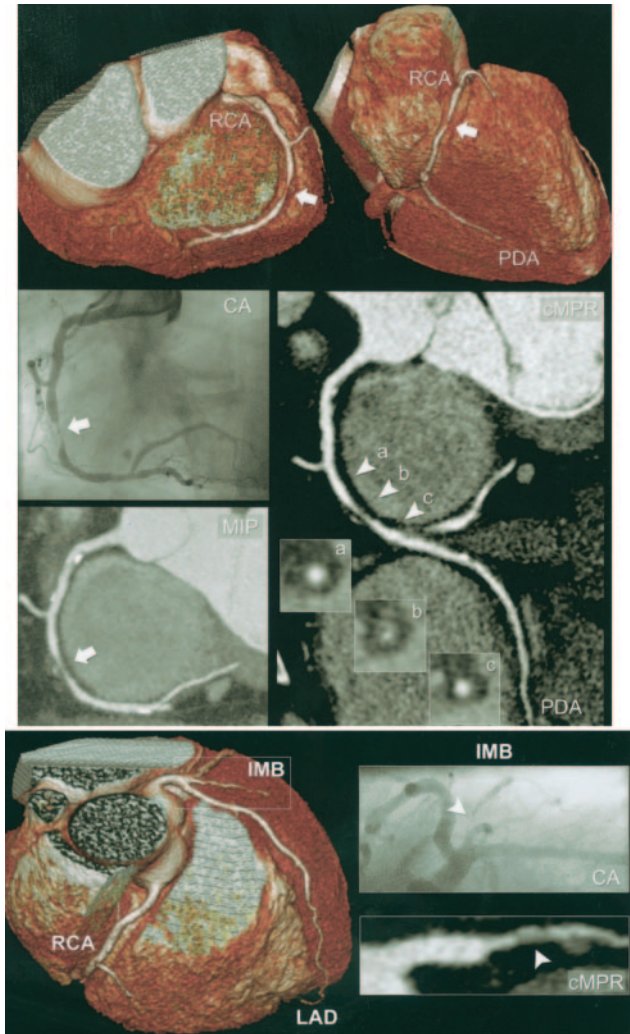


Figure 1. a, CT coronary angiogram and corresponding conventional angiogram of the right coronary artery (RCA) in a patient presenting with stable angina pectoris and a calcium (Agatston) score of 79. The arrow indicates a significant lesion located at the mid RCA. Cross-sectional CT images show a large noncalcific plaque (b) and a normal coronary lumen proximal and distal to the lesion (a, c). Note that the volume-rendered images (colored images) provide an excellent anatomic overview of the coronary arteries but should not be used to score the presence and degree of coronary stenoses. b, Volume-rendered CT image (colored image) providing an overview of the coronary anatomy and showing a small (lumen diameter, 1.5 mm) intermediate branch (IMB). A detailed curved multiplanar reconstructed (cMPR) CT image reveals the presence of a significant stenosis (arrowhead) located at the proximal IMB, which was confirmed on the conventional angiogram (CA). The patient was correctly classified as having 2-vessel disease on the CT scan. MIP indicates maximum-intensity projection; PDA, posterior descending coronary artery; RCA, right coronary artery.

sensitivity and specificity for detecting significant lesions using a 64-slice CT scanner with a rotation time of 375 ms.

The newest 64-slice CT scanners have a shorter rotation time (330 ms) and offer not only a shorter scan time and a higher spatial resolution but also a higher temporal resolution compared with previous scanner generations. Multislice CT coronary angiography of the clinically relevant coronary segments, as designated by the AHA classification, is now

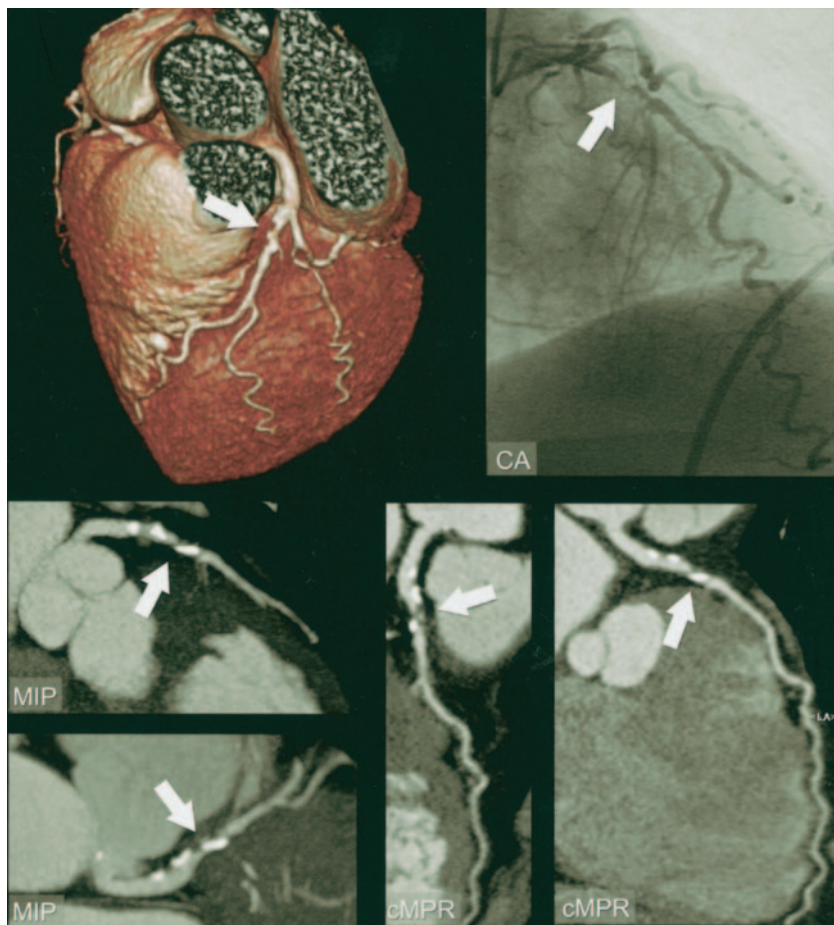


Figure 2. Volume-rendered CT image (colored image) providing an overview of the coronary anatomy and suggesting a significant stenosis of the proximal LAD (indicated by the arrow). More detailed analysis using different CT postprocessing techniques (maximum-intensity projections [MIP] and curved multiplanar reconstructions [cMPR]) confirms the presence of a significant stenosis, which corresponds with the conventional angiogram (CA).

possible. We found that significant coronary stenoses were detected with the latest 64-slice CT scanner with a sensitivity of 99% and a specificity of 95% compared with conventional invasive diagnostic coronary angiography. All but 1 patient with angiographically normal coronary angiograms were correctly identified, rendering the CT technique highly reliable for identifying patients with no significant coronary obstruction. Furthermore, all patients with significant coronary artery disease were correctly diagnosed, and only a single coronary lesion was missed on the CT scan. In addition, we found good agreement between CT coronary angiography and QCA in the classification of patients with no, single-vessel, or multivessel disease. Our results were obtained in patients with a wide spectrum of clinical settings, including atypical chest pain, stable or unstable angina, or non-ST-segment elevation, who had varying degrees of coronary artery disease, ranging from normal coronary angiograms to obstructive disease of 1, 2, or 3 vessels. We did not include patients with ST-segment elevation myocardial infarction; these patients should undergo immediate percutaneous intervention without delay, and the role of CT in these patients is highly questionable. In our study the specificity was somewhat lower because we tended to overestimate the severity of a lesion on the CT scan, resulting in a number of false-positive outcomes, rather than underestimating the lesion severity and thereby “missing” lesions, which may have serious consequences in a symptomatic patient population.

Study Limitations

The estimated radiation dose during CT coronary angiography (15.2 to 21.4 mSv for men and women, respectively) is a cause of concern and is higher than the radiation dose associated with conventional coronary angiography. The radiation exposure can be reduced by technical adjustments such as prospective x-ray tube current modulation. This technique reduces the radiation exposure by $\approx 50\%$ in patients with low heart rates¹⁴ but is sensitive to arrhythmia and limits the possibility of reconstructing data sets during the end-systolic phase. This proved useful in 27% of our patients. Persistent irregular heart rhythm such as atrial fibrillation and frequent extrasystoles preclude multislice coronary angiography. Motion artifacts caused by mild arrhythmia (eg, a single ventricular extrasystole) can be diminished by manual repositioning the reconstruction windows. Severe coronary calcification obscures the coronary lumen and can lead to overestimation of lesion severity because of blooming artifacts, resulting in a lower specificity in patients with high calcium scores. The presence of coronary calcifications also severely limits the applicability of QCA algorithms. In fact, no software able to detect and quantify coronary stenoses has been adequately validated yet.

When evaluating the diagnostic performance of CT coronary angiography on 3 levels (segment by segment, vessel by vessel, and patient by patient), we made repeated assessments within the same patient. However, we performed a sensitivity

analysis after random selection of a single segment per patient and found values that are in line with the values obtained after clustering all available segments. This finding suggests that the nesting of observations within a single patient did not have an important impact on the estimates of the diagnostic performance of CT for detecting significant stenoses in the present study.

Patients with initial heart rates >70 bpm received prescan medication, reducing the mean heart rate to 57 bpm. Future improvements in temporal resolution should diminish motion artifacts related to high heart rates, which could make the administration of prescan β -blockers unnecessary.

Conclusions

Our results show that noninvasive 64-slice CT coronary angiography is a reliable technique to detect coronary stenoses in patients with sinus rhythm presenting with atypical chest pain, stable or unstable angina pectoris, or non-ST-segment elevation myocardial infarction and suggest that this noninvasive technique can now be considered an alternative to invasive diagnostic coronary angiography in selected patients.

References

- Nieman K, Oudkerk M, Rensing BJ, van Ooijen P, Munne A, van Geuns RJ, de Feyter PJ. Coronary angiography with multi-slice computed tomography. *Lancet*. 2001;357:599–603.
- Achenbach S, Giesler T, Ropers D, Ulzheimer S, Derlien H, Schulte C, Wenkel E, Moshage W, Bautz W, Daniel WG, Kalender WA, Baum U. Detection of coronary artery stenoses by contrast-enhanced, retrospectively electrocardiographically gated, multislice spiral computed tomography. *Circulation*. 2001;103:2535–2538.
- Knez A, Becker CR, Leber A, Ohnesorge B, Becker A, White C, Haberl R, Reiser MF, Steinbeck G. Usefulness of multislice spiral computed tomography angiography for determination of coronary artery stenoses. *Am J Cardiol*. 2001;88:1191–1194.
- Vogl TJ, Abolmaali ND, Diebold T, Engelmann K, Ay M, Dogan S, Wimmer-Greinecker G, Moritz A, Herzog C. Techniques for the detection of coronary atherosclerosis: multi-detector row CT coronary angiography. *Radiology*. 2002;223:212–220.
- Kopp AF, Schroeder S, Kuettner A, Baumbach A, Georg C, Kuzo R, Heuschmid M, Ohnesorge B, Karsch KR, Claussen CD. Non-invasive coronary angiography with high resolution multidetector-row computed tomography. Results in 102 patients. *Eur Heart J*. 2002;23:1714–25.
- Nieman K, Cademartiri F, Lemos PA, Raaijmakers R, Pattynama PM, de Feyter PJ. Reliable noninvasive coronary angiography with fast submillimeter multislice spiral computed tomography. *Circulation*. 2002;106:2051–2054.
- Ropers D, Baum U, Pohle K, Anders K, Ulzheimer S, Ohnesorge B, Schlundt C, Bautz W, Daniel WG, Achenbach S. Detection of coronary artery stenoses with thin-slice multi-detector row spiral computed tomography and multiplanar reconstruction. *Circulation*. 2003;107:664–666.
- Kuettner A, Trabold T, Schroeder S, Feyer A, Beck T, Brueckner A, Heuschmid M, Burgstahler C, Kopp AF, Claussen CD. Noninvasive detection of coronary lesions using 16-detector multislice spiral computed tomography technology: initial clinical results. *J Am Coll Cardiol*. 2004;44:1230–1237.
- Mollet NR, Cademartiri F, Nieman K, Saia F, Lemos PA, McFadden EP, Pattynama PM, Serruys PW, Krestin GP, De Feyter PJ. Multislice spiral CT coronary angiography in patients with stable angina pectoris. *J Am Coll Cardiol*. 2004;43:2265–2270.
- Martuscelli E, Romagnoli A, D'Eliseo A, Razzini C, Tomassini M, Sperandio M, Simonetti G, Romeo F. Accuracy of thin-slice computed tomography in the detection of coronary stenoses. *Eur Heart J*. 2004;25:1043–1048.
- Kuettner A, Kopp AF, Schroeder S, Rieger T, Brunn J, Meisner C, Heuschmid M, Trabold T, Burgstahler C, Martensen J, Schoebel W, Selbmann HK, Claussen CD. Diagnostic accuracy of multidetector computed tomography coronary angiography in patients with angiographically proven coronary artery disease. *J Am Coll Cardiol*. 2004;43:831–839.
- Mollet NR, Cademartiri F, Krestin GP, McFadden EP, Arampatzis CA, Serruys PW, De Feyter PJ. Improved diagnostic accuracy with 16-row multislice CT coronary angiography. *J Am Coll Cardiol*. 2005;45:128–132.
- Flohr T, Bruder H, Stierstorfer K, Schaller S. Evaluation of approaches to reduce spiral artifacts in multi-slice spiral CT. Presented at: 89th Scientific Assembly of the Radiological Society of North America; Chicago, Ill; November 28 to December 3, 2004. Abstract.
- Austen WG, Edwards JE, Frye RL, Gensini GG, Gott VL, Griffith LS, McGoon DC, Murphy ML, Roe BB. A reporting system on patients evaluated for coronary artery disease: report of the Ad Hoc Committee for Grading of Coronary Artery Disease, Council on Cardiovascular Surgery, American Heart Association. *Circulation*. 1975;51:5–40.
- Trabold T, Buchgeister M, Kuttner A, Heuschmid M, Kopp AF, Schroeder S, Claussen CD. Estimation of radiation exposure in 16-detector row computed tomography of the heart with retrospective ECG-gating. *Rofo*. 2003;175:1051–1055.
- Agatston AS, Janowitz WR, Hildner FJ, Zusmer NR, Viamonte M Jr, Detrano R. Quantification of coronary artery calcium using ultrafast computed tomography. *J Am Coll Cardiol*. 1990;15:827–832.
- Leschka S, Alkadhi H, Plass A, Desbiolles L, Grunenfelder J, Marinck B, Wildermuth S. Accuracy of MSCT coronary angiography with 64-slice technology: first experience. *Eur Heart J*. 2005;26:1482–1487.

High-Resolution Spiral Computed Tomography Coronary Angiography in Patients Referred for Diagnostic Conventional Coronary Angiography

Nico R. Mollet, Filippo Cademartiri, Carlos A.G. van Mieghem, Giuseppe Runza, Eugène P. McFadden, Timo Baks, Patrick W. Serruys, Gabriel P. Krestin and Pim J. de Feyter

Circulation. 2005;112:2318-2323; originally published online October 3, 2005;
doi: 10.1161/CIRCULATIONAHA.105.533471

Circulation is published by the American Heart Association, 7272 Greenville Avenue, Dallas, TX 75231
Copyright © 2005 American Heart Association, Inc. All rights reserved.
Print ISSN: 0009-7322. Online ISSN: 1524-4539

The online version of this article, along with updated information and services, is located on the
World Wide Web at:

<http://circ.ahajournals.org/content/112/15/2318>

Permissions: Requests for permissions to reproduce figures, tables, or portions of articles originally published in *Circulation* can be obtained via RightsLink, a service of the Copyright Clearance Center, not the Editorial Office. Once the online version of the published article for which permission is being requested is located, click Request Permissions in the middle column of the Web page under Services. Further information about this process is available in the [Permissions and Rights Question and Answer](#) document.

Reprints: Information about reprints can be found online at:
<http://www.lww.com/reprints>

Subscriptions: Information about subscribing to *Circulation* is online at:
<http://circ.ahajournals.org/subscriptions/>